CONF-860675--2

MASTER

REVIEW OF PWR-RELATED THERMAL-SHOCK STUDIES*

R. D. Cheverton

Oak Ridge National Laboratory
Oak Ridge, Tennessee 37831

CONF-860675--2

TI86 011972

S. K. Iskander and D. G. Ball

Computing and Telecommunications Division
Martin Marietta Energy Systems, Inc.

ABSTRACT

Flaw behavior trends associated with pressurized-thermal-shock (PTS) loading of PWR pressure vessels have been under investigation at ORNL for ~12 years. During that time, eight thermal-shock experiments with thick-walled steel cylinders were conducted as a part of the investigations. These experiments demonstrated, in good agreement with linear elastic fracture mechanics (LEFM), crack initiation and arrest, a series of initiation-arrest events with deep penetration of the wall, long crack jumps without significant dynamic effects at arrest, arrest in a rising K_I field, extensive surface extension of an initially short and shallow flaw, and warm prestressing with $\dot{K}_I \leq 0$. This information was used in the development of a fracture-mechanics model that is being used extensively in the evaluation of the PTS issue.

---

*Research sponsored by the Office of Nuclear Regulatory Research, U.S. Nuclear Regulatory Commission under Interagency Agreements 40-551-75 and 40-552-75 with the U.S. Department of Energy under Contract DE-AC05-840R21400 with Martin Marietta Energy Systems, Inc.

DISCLAIMER

1. INTRODUCTION

The pressurized-thermal-shock (PTS) issue has been under intensive investigation by the Nuclear Regulatory Commission (NRC), reactor vendors and utilities since about 1974, and these efforts have recently resulted in the issuance, by the NRC, of a PTS rule [1]. As an aid in formulating the rule, the NRC sponsored the Integrated Pressurized-Thermal-Shock (IPTS) Program, which involved the development of appropriate probabilistic models and the subsequent calculation of the frequency of vessel failure for three specific plants [2-4]. The probabilistic fracture-mechanics model was developed at the Oak Ridge National Laboratory (ORNL), and the validity of the deterministic aspects of this model was established to a large extent on the basis of a series of thermal-shock experiments conducted with thick-walled steel cylinders [5-9]. (These experiments were conducted between 1975 and 1983 as a part of the NRC-sponsored Heavy-Section Steel Technology (HSST) Program [10].) This paper reviews the intent and results of the experiments with regard to development of the fracture-mechanics model for the IPTS studies.

2. ANALYSIS OF PTS TRANSIENTS

A postulated transient of particular interest in the early stages of the HSST thermal-shock program was the large-break loss-of-coolent accident (LBLOCA). It is characterized by (1) rapid depressurization of the primary system, (2) a severe thermal transient (the result of the depressurization and of the subsequent injection of emergency core coolant), and (3) essentially no repressurization. As a consequence of this transient, the belt-line region of the vessel is subjected to severe thermal

shock, and the resultant positive gradient in temperature in the wall of the vessel contributes to positive gradients in the stress intensity factor (K_I), the crack-initiation toughness (K_{Ic}), and the crack-arrest toughness (K_{Ia}), as illustrated in Fig. 1 for a severe-radiation-damage case (end-of-life fluence and "high" concentrations of copper and nickel).

The set of critical-crack-depth curves [7] for the LBLOCA (Fig. 2)* indicates that for the severe-radiation-damage case (1) very shallow flaws can propagate, (2) propagation can consist of a series of initiation-arrest events, (3) rather long crack jumps can take place, (4) warm prestressing [7,11] (WPS, $\dot{K}_I \leq 0$) tends to limit propagation to ~60% of the wall thickness, (5) for WPS to be effective, K ratios (K_I/K_{Ic}) as large as 2.8 must be overcome, (6) even if WPS is effective, a very high value of K_{Ia} is required for arrest prior to WPS, and (7) if WPS were not effective, the flaw would penetrate more than 90% of the wall, but, as indicated in Fig. 1 by the abrupt drop in K_I, would not breach the wall. In addition, as shown in Fig. 3, if crack arrest takes place in the inner half of the wall during a LBLOCA, it must do so with K_I increasing with increasing crack depth.

Transients involving significant repressurization of the primary system result in higher values of and steeper gradients in K_I and introduce the possibility of crack propagation completely through the wall, as indicated in Fig. 4 for a reactor-trip transient [4].

---

*In figures, a = crack depth, w = wall thickness.

When repressurization is initiated after the time corresponding to incipient warm prestressing (IWPS, $\dot{K}_I = 0$), K_I may once again increase with time, but because of load- and temperature-history conditioning of the crack tip the fracture toughness may be elevated above K_{Ic} [11], another phenomenon referred to as warm prestressing. Loading conditions associated with both types of WPS are illustrated in Fig. 5 for a "late"-repressurization PTS transient.

The above analyses were performed using linear elastic fracture mechanics (LEFM) and long (two-dimensional) axially oriented surface flaws. Similar calculations were also made for finite-length surface flaws, and the results indicated that at least in the absence of cladding these flaws would extend on the surface to effectively become long flaws if not limited by higher-toughness regions of the vessel [12]. If the cladding were sufficiently tough, short surface flaws would not extend on the surface and thus if short enough presumably could not extend through the wall.

3. EXPERIMENTAL PROGRAM

The early ORNL analysis of postulated PTS transients indicated a significant potential for severe damage to the reactor pressure vessel in the event of a transient. In addition, as mentioned above, the analysis also revealed that a number of flaw behavior trends were involved that had not been adequately investigated. Thus, an experimental program was in order.

Many of the flaw behavior trends could be and were investigated in experiments involving thermal-shock loading only, while a few required

pressure loading in addition to thermal loading. The scope of the thermal-shock-only experiments included an investigation of all the trends associated with the LBLOCA. Thus far, eight thermal-shock experiments have been conducted. As indicated by the summary of design information (Table 1), all experiments were conducted with large, thick-walled, steel cylinders, each with an intended single, axially oriented, shallow surface flaw. For TSE-2 and TSE-7 the initial intended flaw was semicircular with a radius of ~19 mm, and for the other experiments the initial intended flaw extended the full length of the cylinder and was uniform in depth. All flaws were generated by means of the electron-beam-weld process [13], which introduced the possibility of cross cracks having a surface length of ~6 mm (width of fusion and heat-affected zones) and a depth equal to that of the weld. TSE-5 had an unintended flaw of this type that propagated.

Test cylinders for the first four experiments had a 152-mm wall and a 533-mm outside diameter, and the material was left in the as-quenched condition. The initial temperature of the test cylinder was 288°C, and the thermal shock was applied by pumping a low-temperature mixture of alcohol and water through a narrow coolant gap adjacent to the inner surface. According to the design analysis, this combination of conditions would permit crack initiation (onset of propagation) but not extensive propagation.

To achieve multiple initiation-arrest events and deep penetration, it was necessary to use a test cylinder with a larger ratio of diameter-to-wall thickness. Thus, for the second set of four experiments the outside diameter of the test cylinder was 991 mm, and the wall thickness was

either 152 mm (TSE-5, TSE-5A and TSE-7) or 76 mm (TSE-6). A more severe thermal shock was specified for these experiments so that the test cylinder could also be used in a fully tempered condition. The shock was achieved by contacting the inner surface of the test cylinder, initially at ~100°C, with liquid nitrogen. A special surface coating was used to promote nucleate boiling, which provides the necessary high heat-transfer coefficient [7].

For all of the experiments, extensive instrumentation was used to either directly or indirectly determine wall temperatures and crack depth at the time of each initiation-arrest event. This information was used for an accurate post-test calculation of critical values of K_I corresponding to these events.

4. MATERIALS CHARACTERIZATION STUDIES

An important part of the thermal-shock program was the characterization of the material for each test cylinder. Tensile, Charpy, drop-weight, and fracture toughness (initiation and arrest) data were obtained as an aid in the design and post-test interpretation of the experiments. For instance, the validity of LEFM was judged on the basis of a comparison of calculated critical values of K_I, corresponding to initiation and arrest events, with valid fracture-toughness data (K_{Ic} and K_{Ia}) measured in the lab with the relatively small "standard" specimens (henceforth referred to herein as lab specimens). For this specific purpose, K_{Ic} and K_{Ia} data from additional sources were used to supplement the rather limited amount of valid lab-specimen data for the test-cylinder material. Details of the materials studies are discussed in Ref. 5–9.

5. RESULTS OF EXPERIMENTS

TSE-1: The maximum value of K_I/K_{Ic} was intended to be somewhat less than unity (0.7), and thus fast fracture was not expected. Unstable fracture did not occur, but the crack tip extended ~2 mm in a stable ductile mode as a result of the electron-beam-weld-induced residual stress and low fracture toughness at the crack tip. The absence of fast fracture tended to validate LEFM.

TSE-2: The initial flaw was semicircular, and the maximum value of K_I/K_{Ic} was intended to be greater than unity and to occur close to the surface. Surface extension of the flaw was expected and perhaps radial extension, if the surface extension were sufficient. The flaw extended in surface length from 38 mm to 142 mm in two initiation-arrest events (one at either end). It appeared that additional surface and radial extension were prevented by warm prestressing. This experiment demonstrated crack initiation and arrest in reasonably good agreement with LEFM. However, because of the three-dimensional configuration, uncertainties regarding K_I and warm prestressing were greater than desired.

TSE-3: Not germane to this paper.

TSE-4: The value of $(K_I/K_{Ic})_{max}$ for the "two-dimensional" flaw was intended to be greater than unity (~1.2). An initiation-arrest event took place in good agreement with LEFM.

TSE-5: A series of three initiation-arrest events with deep penetration (80% of the wall) of the two-dimensional flaw occurred in good agreement with LEFM. Two unintended events, a long crack jump and extensive propagation of an inadvertent small cross crack, indicated that

dynamic effects at arrest were negligible, and that an initially short crack, at least in the absence of cladding, could extend in surface length to effectively become a long flaw.

TSE-5A: A series of four initiation-arrest events with ~50% penetration of the wall was intended and occurred in good agreement with LEFM. A fifth event was prevented by warm prestressing, and one of the four arrest events took place with K_I increasing with crack depth (dK_I/da = 0.3 MPa $\sqrt{m}$/mm), as was expected. At the time of IWPS ($\dot{K}_I = 0$), the value of K_I was 152 MPa $\sqrt{m}$, and following IWPS, a maximum K ratio of 2.3 was achieved without crack initiation taking place.

TSE-6: The smaller wall thickness for this experiment (76 compared to 152 mm) introduced a potential for a single long crack jump to a depth greater than 90% of the wall thickness. There were actually two initiation arrest events, the first being relatively short, with a total penetration of 93%. This helped to demonstrate the inability of a long flaw to fully penetrate the vessel wall under thermal-shock loading conditions only. Furthermore, once again there appeared to be negligible dynamic effects associated with arrest following a long crack jump, and the first arrest event took place with K_I increasing with crack depth (dK_I/da = 0.8 MPa $\sqrt{m}$/mm).

TSE-7: This experiment was intended to demonstrate once again the ability of a short and shallow flaw, in the absence of cladding, to extend on the surface to effectively become a long flaw. The initial flaw was oriented axially and was essentially semielliptical in shape with a surface length of 37 mm and a depth of 14 mm. In a single event the flaw extended on the surface, bifurcating many times, to produce almost the

entire cracking pattern shown in Fig. 6. Following this event, there were two more that extended the complex flaw radially to depths of ~55 mm in the central portion of the cylinder and to lesser depths toward the ends of the cylinder. (The second event also extended the surface length somewhat.) A fourth event was prevented by warm prestressing.

6. DISCUSSION OF RESULTS

Critical values of K_I deduced from the thermal-shock experiments and corresponding to the crack initiation and arrest events are compared with lab-specimen data and data from a French thermal-shock experiment [14] in Figs. 7 and 8. It is apparent that all of the test-cylinder K_{Ic} data points, with the exception of one of the French points, are above the ASME lower-bound curve and, with the exception of two points, are below an approximate upper bound of the K_{Ic} data that were used to generate the ASME lower-bound curve [15]. (The test-cylinder lab-specimen K_{Ic} data correspond to $T - RT_{NDT} \leq -65°C$ and have essentially the same upper and lower bounds as the ASME data.)

Figure 8 includes, in addition to the ORNL and French data and the ASME K_{IR} curve, the 5th and 95th percentile curves corresponding to a Battelle-Columbus Laboratories lab-specimen K_{Ia} data base [16,17] which consists of 233 data points for A533 and A508 material, including 25 points obtained from the thermal-shock test-cylinder characterization studies. As indicated by Fig. 8, the scatter in the lab-specimen data is approximately ±45%, and only a small fraction of the data points falls below the K_{IR} curve. All of the K_{Ia} values deduced from the ORNL thermal-shock experiments fall within the lab-specimen scatter band and well

above the K_{IR} curve, while the three French data points cluster about the K_{IR} curve.

A comparison of the ORNL and French data is of interest because the experiments were very similar. The test cylinders were similar in size and material and were both thermally loaded by quenching in liquid nitrogen. However, the French fracture surfaces were very flat and free of unbroken ligaments [14], while the ORNL surfaces were relatively rough and, in some cases, as shown in Fig. 9, had many unbroken ligaments. Since the restraining force of the ligaments was not accounted for in the calculation of critical values of K_I, the existence of ligaments on the ORNL surfaces could be a reason for the generally higher indicated values of fracture toughness relative to the French values.

The two data points in Fig. 8 that correspond to arrest in a rising K_I field fall well within the scatter band of the lab-specimen data. This indicates that the critical value of K_I for arrest in a rising K_I field is about the same as that for a falling K_I field ($dK_I/da < 0$), which is the usual condition when obtaining lab-specimen K_{Ia} data. It should be noted, however, that the values of dK_I/da (0.3 and 0.8 MPa $\sqrt{m}$/mm) were somewhat less than the maximum calculated for the LBLOCA (1.8 MPa $\sqrt{m}$/mm for $K_I < 220$ MPa $\sqrt{m}$).

The large scatter in the lab-specimen and in the test-cylinder K_{Ic} and K_{Ia} data tend to preclude drawing conclusions regarding the validity of LEFM for thermal-shock loading conditions. However, if one accepts the apparent fact that both very large and lab-sized specimens can exhibit large scatter in valid fracture-toughness data, then the coincidence of the scatter bands and a lack of significant anomalies during

the thermal-shock experiments indicate that LEFM is valid, at least for (T — RTNDT) < 20°C for crack-initiation events and (T — RTNDT) < 60°C for crack-arrest events.

The data in Fig. 8 indicate that dynamic effects at arrest were negligible. If dynamic effects were substantial, the static analysis would tend to yield low values of K_{Ia}. As indicated by Fig. 8, the statically calculated values for the two long crack jumps (second arrest events for TSE-5 and TSE-6) are high rather than low (just below the upper bound of the lab-specimen data).

Warm prestressing with $\dot{K}_I < 0$ may have prevented reinitiation in each of the ORNL thermal-shock experiments. However, only in the case of TSE-5A was the calculated best estimate of $(K_I/K_{Ic})_{max}$ for the final crack depth large enough to account for the uncertainties in the experiment and analysis. The calculated best estimate of $(K_I/K_{Ic})_{max}$ (max with respect to time), was 2.3. With reference to Fig. 7, it can be seen that a factor of 2.3 more than accommodates the upper bound of the K_{Ic} data. Thus, warm prestressing with $\dot{K}_I < 0$ was demonstrated in a convincing manner. It is of interest to note, however, that the TSE-5A K_I value corresponding to $\dot{K}_I = 0$ (152 MPa $\sqrt{m}$) was somewhat less than calculated for the LBLOCA (Fig. 2) and for another severe PTS transient (Fig. 4).

Results of the thermal-shock experiments conducted thus far have provided sufficient confidence in the validity of LEFM for PTS loading conditions and over a wide enough range of K_I and dK_I/da values to permit development of an LEFM model [2-4,18,19] for use as an aid in evaluating PWR vessel integrity during PTS transients [2-4]. The question

of validity of WPS and arrest in a rising K_I field at K_I values larger than those achieved in the experiments was avoided by specifying a maximum value of K_{Ia} equal to 220 MPa $\sqrt{m}$, in which case the attainment of higher calculated values of K_I resulted in a prediction of vessel failure. Furthermore, the possibility that the cladding would restrict surface extension of initially short flaws was ignored.

Although the above fracture-mechanics model was considered reasonable for the IPTS studies, additional experiments [20-24] are planned and are under way with an objective of perhaps being able to take more credit for WPS, cladding effects and crack arrest.

References

1. *Federal Register*, Vol. 50, No. 141, July 23, 1985, Section 50.61, "Fracture Toughness Requirements for Protection Against Pressurized Thermal Shock Events," pp. 29937–29945.

2. T. J. Burns et al., *Pressurized Thermal Shock Evaluation of the Oconee-1 Nuclear Power Plant*, NUREG/CR-3770 (ORNL/TM-9176), draft, April 13, 1984.

3. D. L. Selby et al., *Pressurized Thermal Shock Evaluation of the Calvert Cliffs Unit 1 Nuclear Power Plant*, NUREG/CR-4022 (ORNL/TM-9408), Sept. 1985.

4. D. L. Selby et al., *Pressurized Thermal Shock Evaluation of the H. B. Robinson Unit 2 Nuclear Power Plant*, NUREG/CR-4183 (ORNL/TM-9567), Vols. 1 and 2, Sept. 1985.

5. R. D. Cheverton, *Pressure Vessel Fracture Studies Pertaining to a PWR LOCA-ECC Thermal Shock: Experiments TSE-1 and TSE-2*, ORNL/NUREG/TM-31, Sept. 1976.

6. R. D. Cheverton and S. E. Bolt, *Pressure Vessel Fracture Studies Pertaining to a PWR LOCA-ECC Thermal Shock: Experiments TSE-3 and TSE-4 and Update of TSE-1 and TSE-2 Analysis*, ORNL/NUREG-22, Dec. 1977.

7. R. D. Cheverton et al., *Pressure Vessel Fracture Studies Pertaining to the PWR Thermal-Shock Issue: Experiments TSE-5, TSE-5A and TSE-6*, NUREG/CR-4249 (ORNL-6163), June 1985.

8. R. D. Cheverton et al., *Pressure Vessel Fracture Studies Pertaining to the PWR Thermal-Shock Issue: Experiment TSE-7*, NUREG/CR-4304 (ORNL-6177), Aug. 1985.

9. R. D. Cheverton et al., "Fracture Mechanics Data Deduced from Thermal-Shock and Related Experiments with LWR Pressure Vessel Material," *Journal of Pressure Vessel Technology*, 102/Vol. 105, May 1983.

10. G. D. Whitman, *Historical Summary of the Heavy-Section Steel Technology Program and Some Related Activities in Light-Water Reactor Pressure Vessel Safety Research*, NUREG/CR-4489 (ORNL-6259), March 1986.

11. F. J. Loss, A. A. Gray, Jr., and J. R. Hawthorne, *Significance of Warm Prestress to Crack Initiation During Thermal Shock*, NRL/NUREG-8165, Naval Research Laboratory, Washington, DC, Sept. 1977.

12. R. D. Cheverton and D. G. Ball, "A Reassessment of PWR Pressure Vessel Integrity During Overcooling Accidents, Considering 3-D Flaws," *Journal of Pressure Vessel Technology*, Vol. 106/375, November 1984.

13. P. P. Holz, "Preparation of Long Axial Flaw for TSE-5A," pp. 35–37 in *Heavy-Section Steel Technology Program Quart. Prog. Rep. July-September 1980*, NUREG/CR-1806 (ORNL/NUREG/TM-419), Dec. 1980.

14. A. Pellissier-Tanon, P. Sollogoub, and B. Houssin, "Crack Initiation and Arrest in an SA 508 Class-3 Cylinder Under Liquid Nitrogen Thermal-Shock Experiment," in *Transactions of the 7th International Conference on Structural Mechanics in Reactor Technology*, Vols. G and H, North Holland Publishing Co., Aug. 1983.

15. *ASME Code*, Section XI, Division 1, Subsection NB-2331.

16. A. R. Rosenfield, "Validation of Compact-Specimen Crack-Arrest Data," *Technical Briefs, Journal of Engineering Materials and Technology*, 106/207 (1984).

17. A. R. Rosenfield et al., *Heavy-Section Steel Technology Program Semiannual Progress Report October–March FY 1984*, Oak Ridge Natl. Lab. (1984).

18. R. D. Cheverton and D. G. Ball, *OCA-P, A Deterministic and Probabilistic Fracture-Mechanics Code for Application to Pressure Vessels*, NUREG/CR-3618 (ORNL-5991), May 1984.

19. D. G. Ball and R. D. Cheverton, *Adaptation of OCA-P, a Probabilistics Fracture-Mechanics Code, to a Personal Computer*, NUREG/CR-4468 (ORNL/CSD/TM-233), January 1986.

20. R. D. Cheverton et al., "Thermal-Shock Technology," *Heavy-Section Steel Technology Program Semiannual Progress Report for April–September 1985*, NUREG/CR-4219, Vol. 2 (ORNL/TM-9593/V2), pp. 182–192.

21. R. H. Bryan et al., *Pressurized-Thermal-Shock Test of 6-in.-Thick Pressure Vessels. PTSE-1: Investigation of Warm Prestressing and Upper-Shelf Arrest*, NUREG/CR-4106 (ORNL-6235), April 1985.

22. W. R. Corwin et al., *Effects of Stainless Steel Weld Overlay Cladding on the Structural Integrity of Flawed Steel Plates in Bending, Series 1*, NUREG/CR-4015 (ORNL/TM-9390), April 1985.

23. W. R. Corwin et al., *Charpy Toughness and Tensile Properties of Neutron Irradiated Stainless Steel Submerged-Arc Weld Cladding Overlay*, NUREG/CR-3927 (ORNL/TM-9309), September 1984.

24. B. R. Bass, C. E. Pugh and H. K. Stamm, "Dynamic Analysis of a Crack Run-Arrest Experiment in a Nonisothermal Plate," *Proceedings of the 1985 Pressure Vessel and Piping Conference*, PVP - Vol. 98-2, ASME.

Table 1. Summary of test conditions for ORNL thermal-shock experiments

Parameter	Experiment						
	TSE-1	TSE-2	TSE-4	TSE-5	TSE-5A	TSE-6	TSE-7
Cylinder dimensions, mm							
Outside diameter	533	533	533	991	991	991	991
Wall thickness	152	152	152	152	152	76	152
Length	914	914	914	1220	1220	1220	1220
Cylinder Material							
Designation	A508, class-2 chemistry						
Tempering temperature, deg C	As quenched →			613	679	613	704
RTNDT, deg C	75	75	75	66	10	66	−1
Flaw (initial)							
Orientation	Axial →						
Length, mm	914	38	914	1220	1220	1220	37
Depth, mm	11	19	11	16	11	7.6	14
Thermal shock							
Initial temp. of cylinder, deg C	288	288	288	96	96	96	96
Initial temp. of coolant, deg C	4	−23	−25	−320	−320	−320	−320
Quench medium	Water/alcohol →			LN_2	LN_2	LN_2	LN_2

Figure Captions

Fig. 1. Typical instantaneous temperature, stress, fluence, stress-intensity factor, and fracture-toughness distributions through wall of PWR vessel during LBLOCA (long axial flaw; "high" copper, nickel, and fluence; t = 4 min).

Fig. 2. Critical-crack-depth curves for LBLOCA.

Fig. 3. K_I vs a/w for LBLOCA.

Fig. 4. Critical-crack-depth curves for a reactor-trip transient.

Fig. 5. Warm prestress phenomena associated with a PTS transient.

Fig. 6. Developed view of inner surface of TSE-7 test cylinder showing final crack pattern.

Fig. 7. Comparison of lab-specimen and large-specimen (test-cylinder) K_{Ic} data.

Fig. 8. Comparison of lab-specimen and large-specimen (test-cylinder) K_{Ia} data.

Fig. 9. TSE-5A fracture surface showing rough texture and unbroken ligaments.

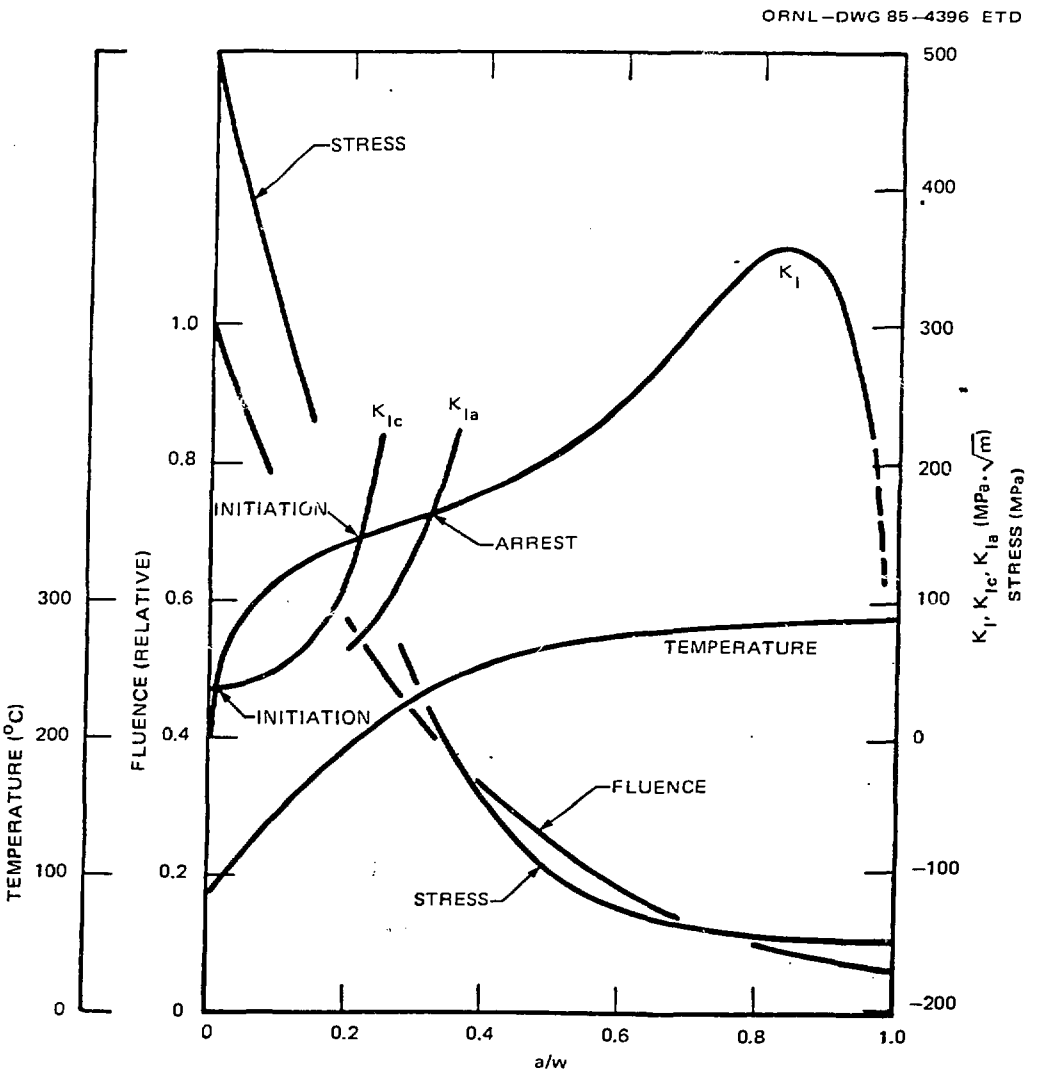

Fig. 1. Typical instantaneous temperature, stress, fluence, stress-intensity factor, and fracture-toughness distributions through wall of PWR vessel during LBLOCA (long axial flaw; "high" copper, nickel, and fluence; t = 4 min).

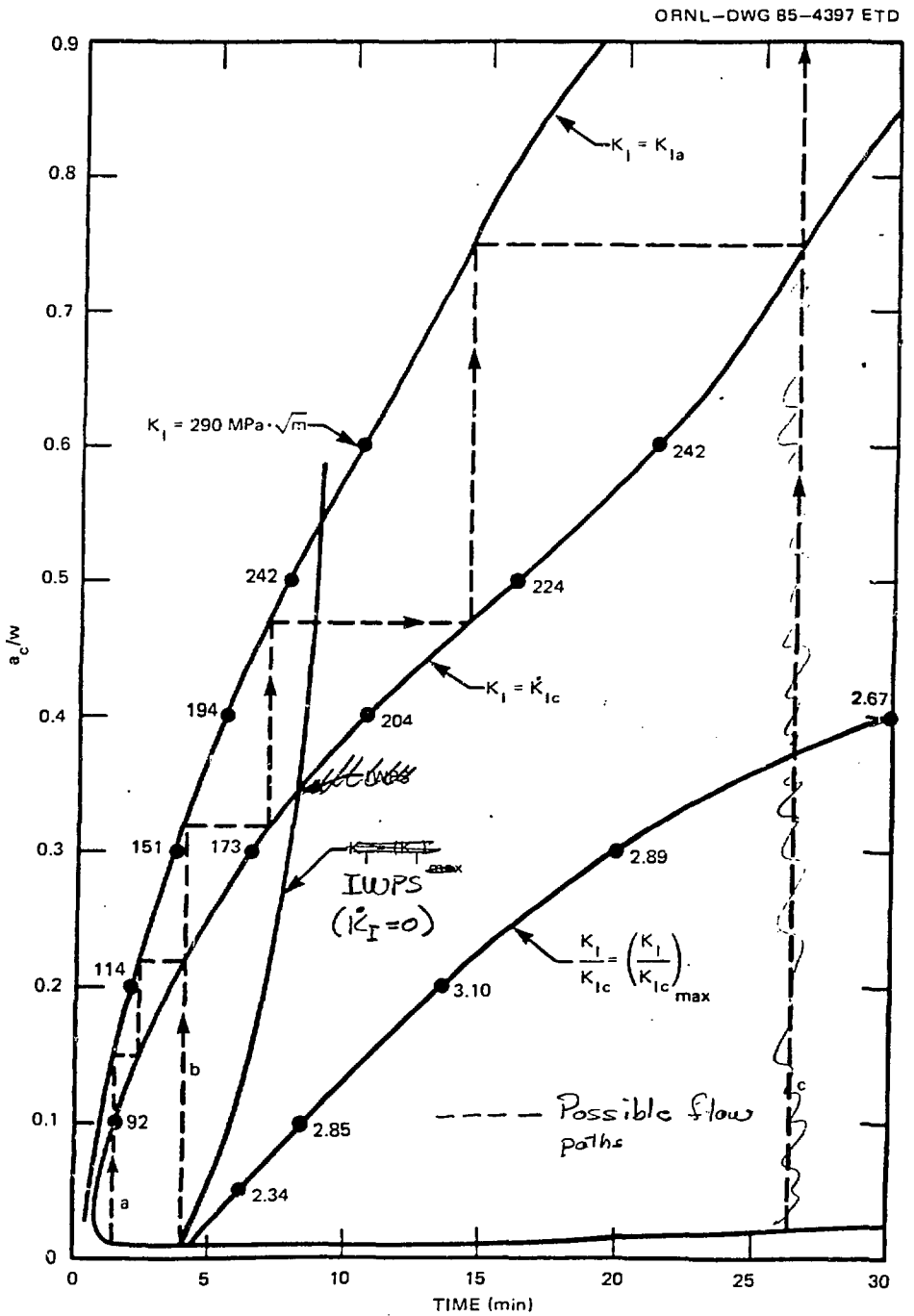

Fig. 2. Critical-crack-depth curves for LBLOCA.

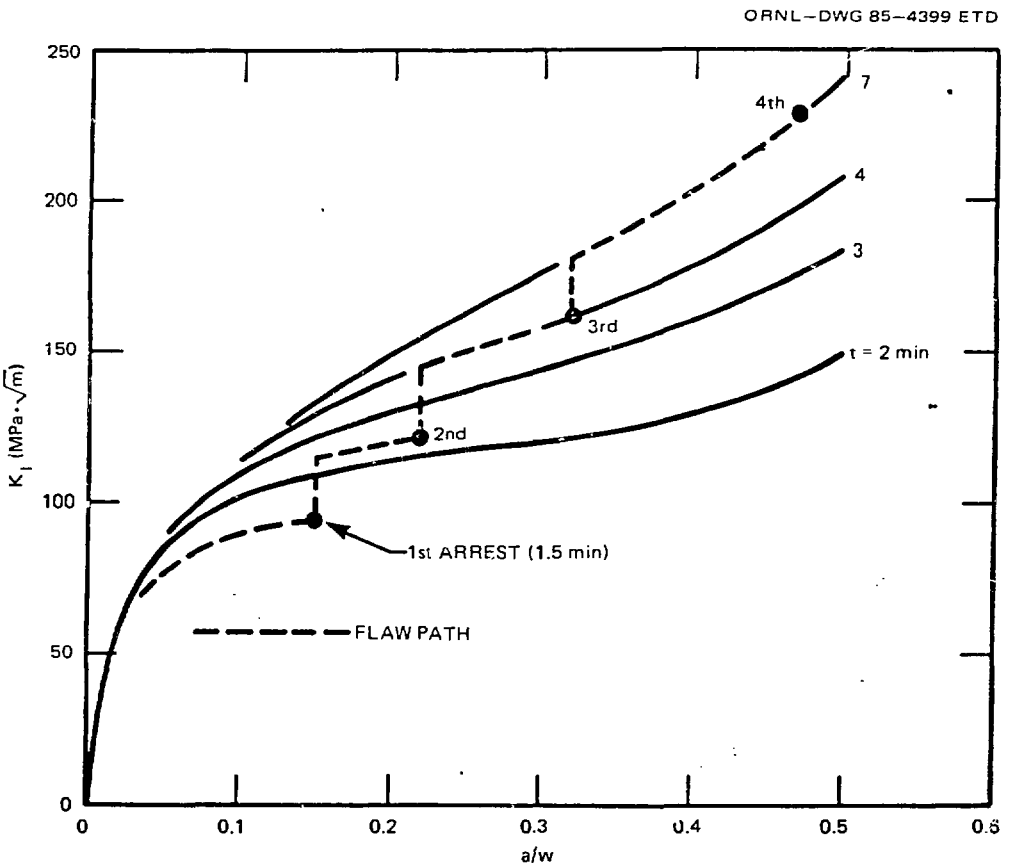

Fig. 3. K_I vs a/w for LBLOCA.

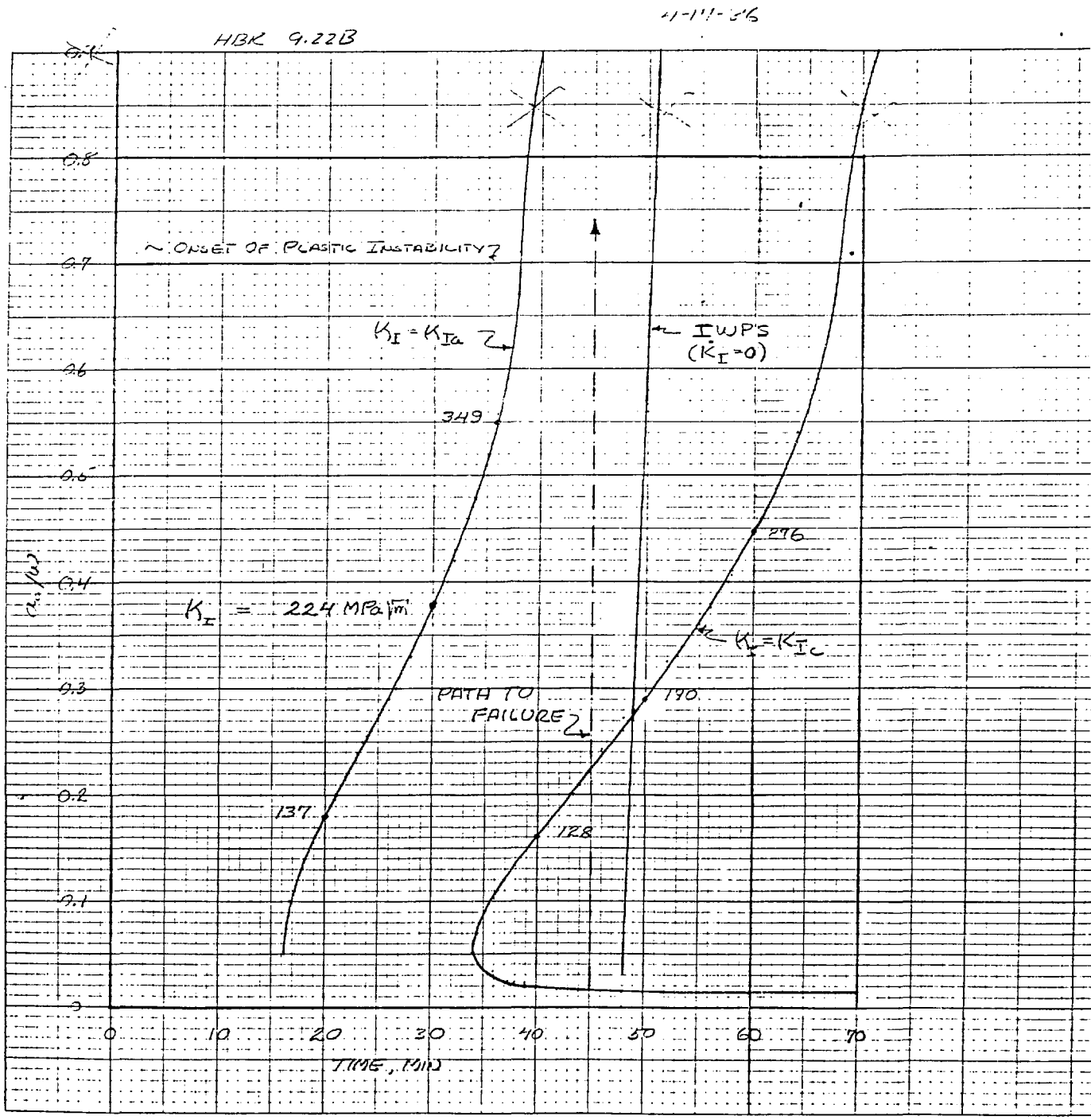

Fig. 4. Critical-crack-depth curves for a reactor-trip transient.

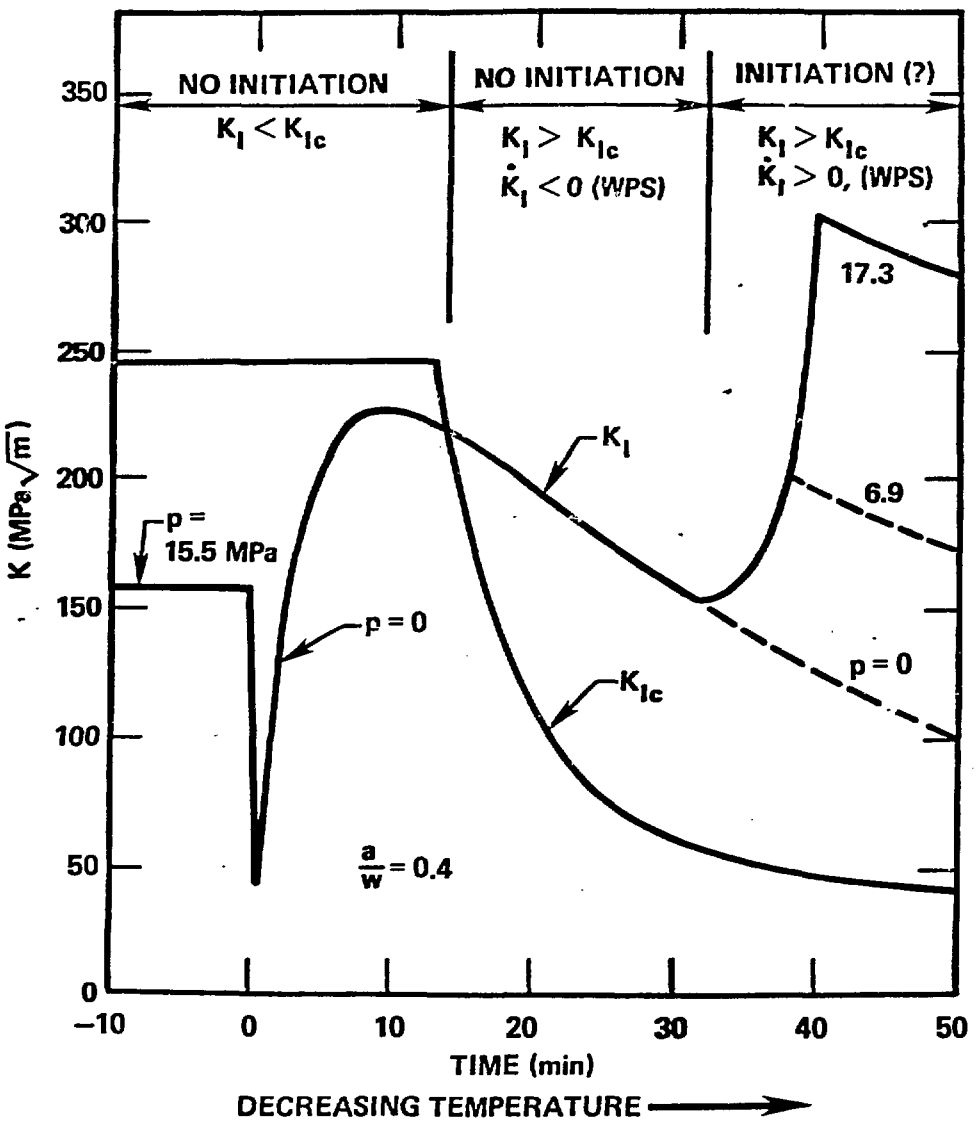

Fig. 5. Warm prestress phenomena associated with a PTS transient.

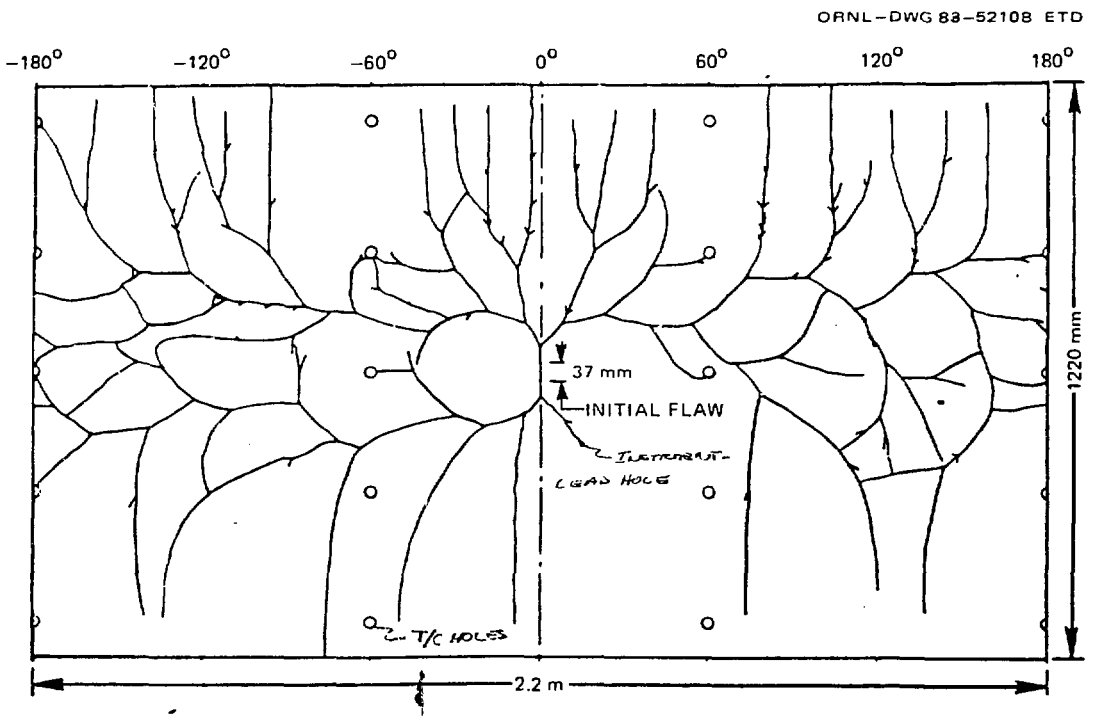

Fig. 6. Developed view of inner surface of TSE-7 test cylinder showing final crack pattern.

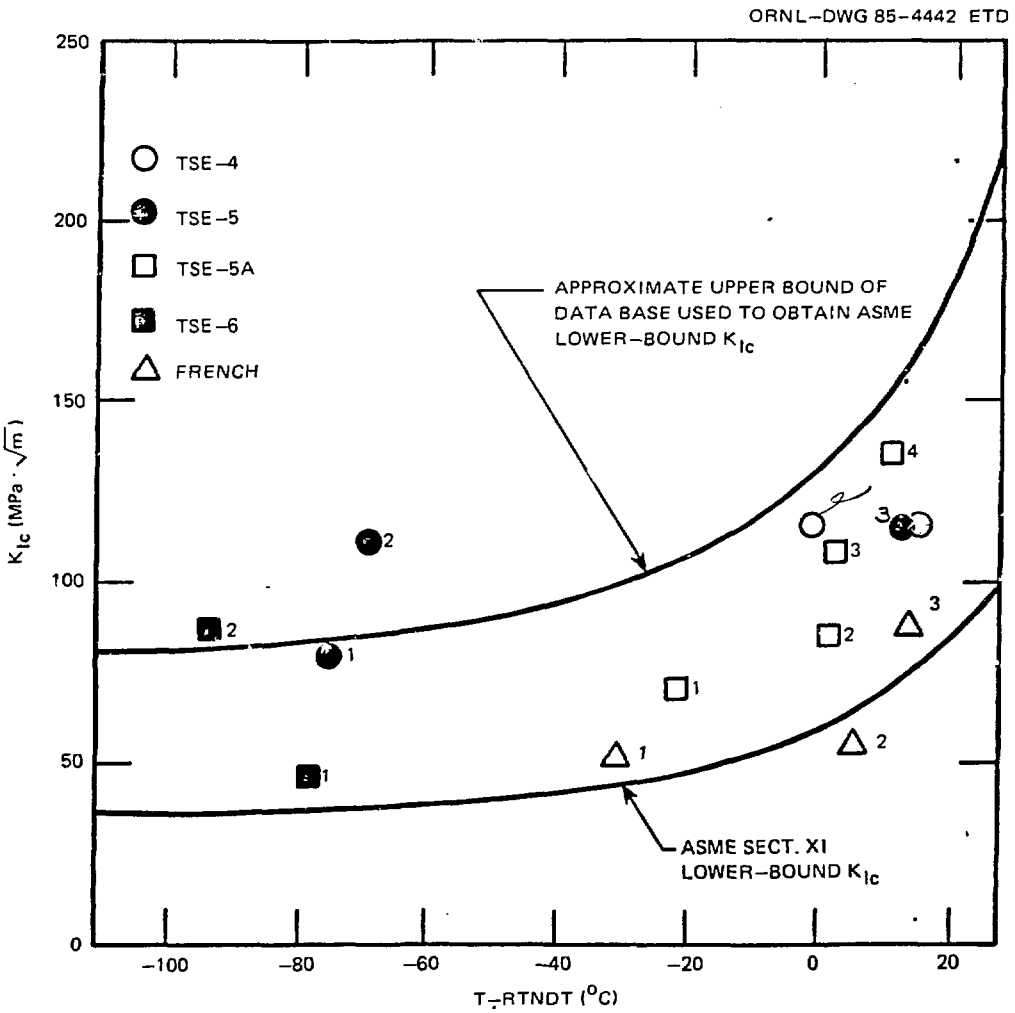

Fig. 7. Comparison of lab-specimen and large-specimen (test-cylinder) K_{Ic} data.

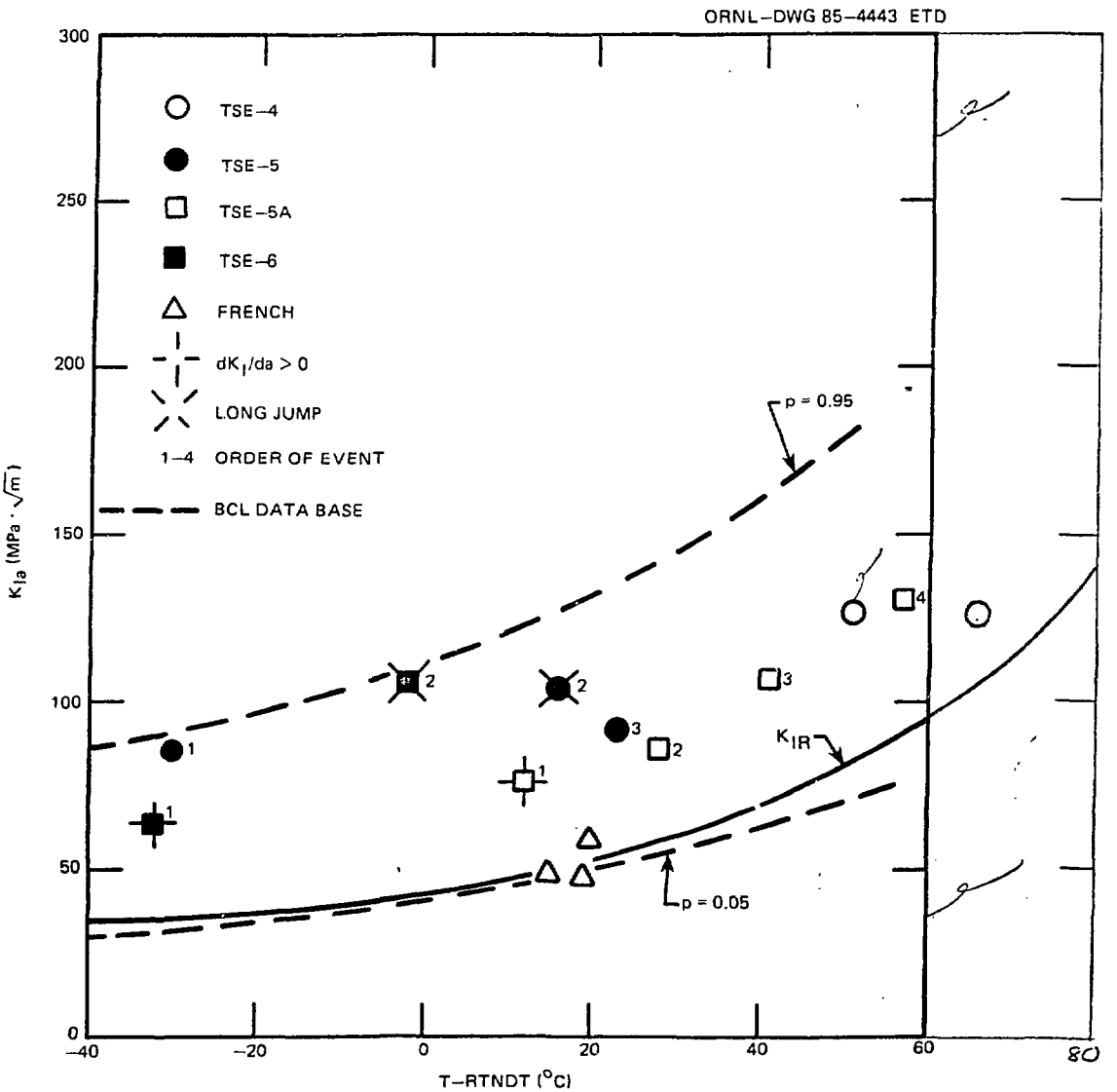

Fig. 8. Comparison of lab-specimen and large-specimen (test-cylinder) K_{Ia} data.

M&C PHOTO Y175292A

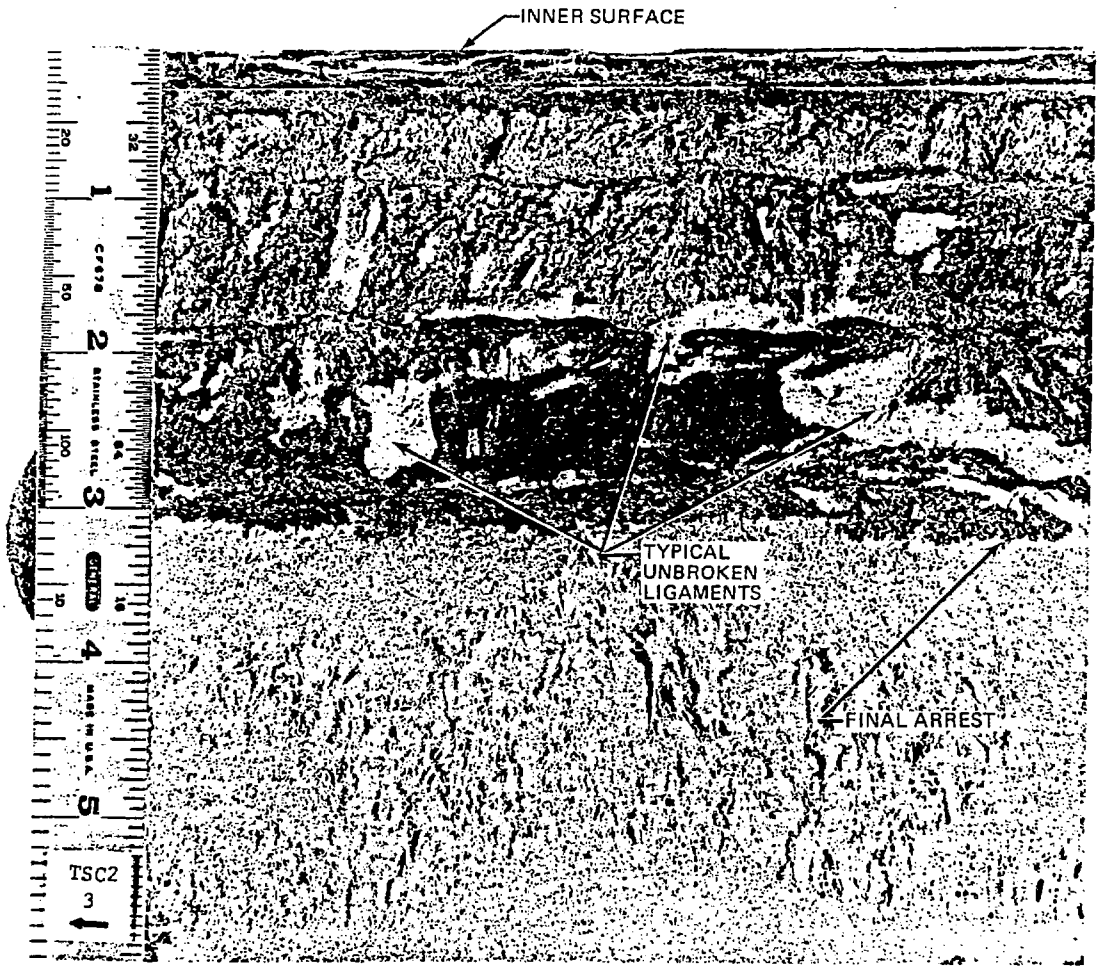

Fig. 9. TSE-5A fracture surface showing rough texture and unbroken ligaments.